Soil Dynamics and Earthquake Engineering 30 (2010) 1319–1328

Contents lists available at ScienceDirect

Soil Dynamics and Earthquake Engineering

journal homepage: www.elsevier.com/locate/soildyn

Seismic microzonation and earthquake damage scenarios for urban areas

Atilla Ansal*, Aslı Kurtuluş, Gökçe Tönük

Bogaziçi University, Kandilli Observatory and Earthquake Research Institute, Çengelköy, 34684 Istanbul, Turkey

ARTICLE INFO

Article history:
Received 23 July 2009
Received in revised form
29 May 2010
Accepted 12 June 2010

ABSTRACT

A methodology for seismic microzonation and earthquake damage scenarios may be considered as composed of two stages. In the first stage, microzonation maps with respect to estimated earthquake characteristics on the ground surface are generated for an investigated urban area. The effects of local geological and geotechnical site conditions are taken into account based on site characterization with respect to representative soil profiles extending down to the engineering bedrock. 1D site response analyses are performed to calculate earthquake characteristics on the ground surface using as many as possible, hazard compatible real acceleration time histories. In the second stage, vulnerability of buildings and pipeline systems are estimated based on site-specific ground motion parameters. A pilot study is carried out to evaluate seismic damage in a district in Istanbul, Turkey. The results demonstrate the significance of site characterization and site response analysis in calculating the earthquake characteristics on the ground surface in comparison to simplified empirical procedures.

1. Introduction

Seismic microzonation and earthquake loss estimation scenarios are among the essential tools needed for city planning, disaster preparedness, risk reduction, hazard mitigation decisions, and urban rehabilitation actions in earthquake prone areas. Loss estimation due to possible future earthquakes in an urban environment is a very complex process that requires detailed building and lifeline inventories, probabilistic or deterministic analyses of seismic hazard on the ground surface and assessment of vulnerability of the inventories due to the estimated earthquake characteristics. There are basically three phases that control the earthquake damage estimation process: (1) seismic hazard assessment and input ground motion characteristics, (2) modification of these input ground motion due to site conditions, and (3) vulnerability formulations to estimate damage distribution. All these three stages could play significant role on the outcome, depending how they are evaluated.

Several methodologies [1–5] have been developed over the past years that take into account various aspects of loss estimation process. However, none of these loss estimation methodologies involves detailed analysis of local site conditions when predicting ground motion characteristics on the ground surface. The methodology proposed in this work provides a loss estimation method that takes local site effects into account by performing large numbers of 1D site response analyses using Shake91 code [6].

A software tool is developed to apply this methodology for damage scenario predictions in urban areas. In order to analyze the complex process for conducting microzonation with respect to different earthquake characteristics on the ground surface and to calculate damage distributions within the investigated urban environment, it is essential to utilize a flexible software package. The main purpose of such an earthquake scenario software tool besides performing microzonation and earthquake damage scenarios for the investigated area is to have the capability to conduct parametric studies for evaluating the range of variability induced in these three stages and to assess the significance of the related factors in the estimated final damage distributions.

2. Methodology for microzonation and damage scenarios

The proposed methodology is composed of two main phases. The first phase involves generation of microzonation maps with respect to earthquake ground shaking parameters due to the selected regional earthquake hazard scenario. In the second phase, vulnerability of buildings and pipelines are estimated based on the calculated earthquake ground shaking parameters. Results are displayed in damage distribution maps for buildings and pipeline systems that are produced in GIS environment.

The first step is to adopt a grid system that divides the investigated urban area into cells (typically 250 m × 250 m) according to the availability of geological, geophysical, and geotechnical data. Variations of earthquake shaking parameters

* Corresponding author.
E-mail address: ansal@boun.edu.tr (A. Ansal).

0267-7261/$ - see front matter © 2010 Elsevier Ltd. All rights reserved.
doi:10.1016/j.soildyn.2010.06.004

for bedrock outcrop within the area are separately determined for a specified level of exceedance probability or using deterministic simulations. Site characterization is performed based on available borings and other relevant information by defining one representative soil profile for each cell with shear wave velocities extending down to the engineering bedrock (shear wave velocity, $V_s \geq 750$ m/s).

Site specific earthquake characteristics on the ground surface for each representative soil profile are calculated using one dimensional site response analyses, Shake91. Hazard compatible acceleration time histories (in terms of expected fault type, fault distance, and earthquake magnitude) are selected and site response analyses are performed for a selected number of acceleration time histories. It was demonstrated by Ansal and Tönük [7] that if limited number of input acceleration time histories (e.g. 3 records as specified in some earthquake codes) are used, even with scaling to the same peak ground acceleration (PGA) amplitudes for site response analysis, the results in terms of PGA, peak ground velocity (PGV), and elastic acceleration response spectrum (SA) can be significantly different for different sets of input motion records. This would introduce an important uncertainty when estimating the damage distribution. Therefore to partially overcome this issue, one possible option is to use as many acceleration time histories as possible (e.g. 25–30) from the hazard compatible bin (in terms of fault type, earthquake magnitude, and epicenter distance) as input motions for site response analyses. The selected time histories can be real earthquake acceleration records, or alternatively can be calculated using simulation models [8]. In the case of using real acceleration time histories, PGA scaling is adopted as suggested by Ansal et al. [9] and Durukal et al. [10].

Site response analyses using Shake91 provide the variations of PGA and SA on the ground surface. Variation of PGV is determined through integration of acceleration time histories on the ground surface. Average of all spectral acceleration values between 0.1 and 1.0 s periods of the elastic acceleration response spectrum (SA_{avg} (0.1–1 s)) is calculated as one parameter representing earthquake shaking intensity on the ground surface. Site-specific peak spectral accelerations corresponding to 0.2 s ($SA_{Borcherdt}$) are also calculated through empirical relationship proposed by Borcherdt [11] using equivalent (average) shear wave velocities for the top 30 m of soil profiles (V_{s30}). Superposition of empirically

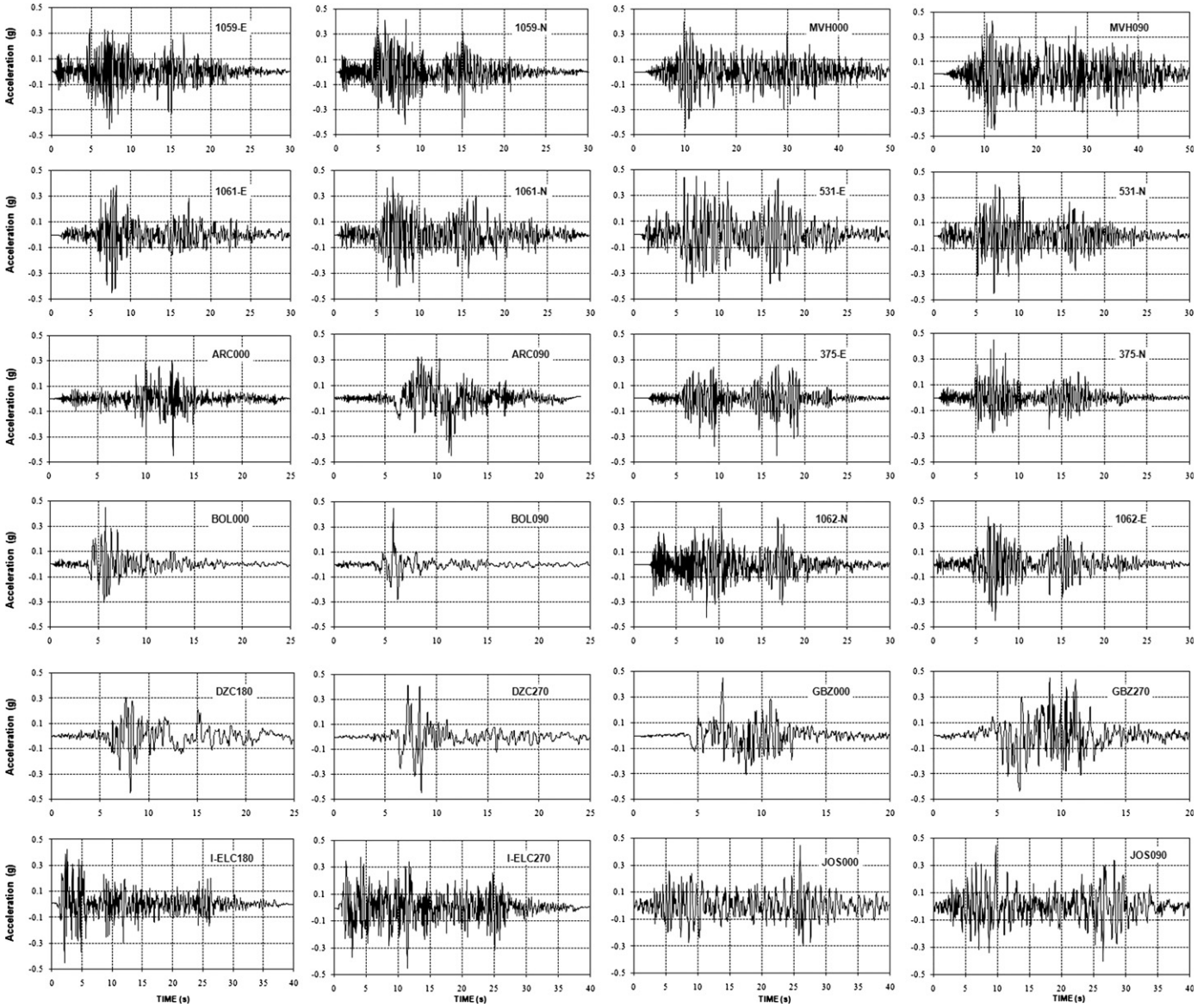

Fig. 1. Acceleration time histories that are used as input motion in site response analysis.

calculated values (i.e. $SA_{Borcherdt}$) with those calculated using Shake91 (e.g. SA_{avg} (0.1–1 s)) provides a general assessment of the variation of site effects and is used as a parameter for microzonation with respect to ground shaking intensity [12].

In order to assess seismic vulnerability for buildings, two parameters; site-specific short period (corresponding to 0.2 s) and long period (corresponding to 1 s) spectral accelerations are calculated. Site-specific acceleration response spectrum is used to determine spectral accelerations for the short period (S_s) and for the long period (S_l). An approach is adopted to determine the best-fit NEHRP [13] envelope to the calculated average acceleration response spectra [14]. All the requirements of the NEHRP design spectra are applied in obtaining the short (S_s) and long (S_l) period spectral accelerations. The two independent variables in the developed optimization algorithm are S_s and S_l. The NEHRP design spectrum is preferred because of its flexibility in defining spectral accelerations [15].

At this stage, microzonation maps for the investigated urban area may be prepared with respect to V_{s30}, NEHRP site classification, PGA, PGV, $SA_{avg\ (0.1-1\ s)}$, $SA_{Borcherdt}$, S_s, and S_l. A map representing the ground-shaking intensity is prepared where the estimated relative shaking intensity levels are based on the superposition of two parameters: SA_{avg} (0.1–1 s) and $SA_{Borcherdt}$. The approach adopted in the assessment of the calculated microzonation maps using SA_{avg} (0.1–1 s) and $SA_{Borcherdt}$, involves the division of the area into three zones as A, B, and C [16]. Since the site characterizations, as well as all the analysis performed, require various approximations and assumptions, it is preferred not to present the numerical values for the microzonation parameters. The variations of the parameters are considered separately and their frequency distributions are calculated to determine the boundaries between the three zones. The zone C shows the most unsuitable 33 percentile (e.g. high spectral accelerations), zone B the medium 34 percentile and zone A shows the most favorable 33 percentile (e.g. low spectral accelerations). The final microzonation map is a relative map defined in terms of three zones independent of the absolute values of the ground shaking intensity.

In the second phase of the procedure, vulnerability analyses for building and pipeline inventories are evaluated. Site-specific spectral accelerations S_s and S_l are used to assess the vulnerability of the building stock. The analytical estimation of structural damage is formulated based on [1], where the vulnerability relationships (also called fragility curves) are developed in terms of spectral displacements, which in turn are calculated from the estimated mean inelastic drift capacities of buildings for various damage states. The mean drift demand of a typical building is estimated through nonlinear static procedures (NSPs), which are based on performance-based seismic evaluation [17–19]. NSPs are based on the capacity (pushover) curve of the given building and the estimation of the inelastic spectral displacement demand consistent with the capacity curve.

In spectral displacement-based fragility curves, the horizontal axis represents the spectral displacement demand and vertical axis refers to the cumulative probability of structural damage reaching or exceeding the threshold of a given damage state. The analytical expression of each fragility curve is based on the assumption that earthquake damage distribution can be represented by a lognormal distribution function [1,20]:

$$P[D \geq d_s | S_{di}] = \Phi[(1/\beta_{ds}) \ln(S_{di}/S_{d,ds})] \quad (1)$$

where D refers to the damage, S_{di} is the inelastic spectral displacement demand, $S_{d,ds}$ represents the median value of spectral displacement corresponding to the threshold of the damage state, d_s (slight, moderate, extensive or complete), reached, β_{ds} is the standard deviation of the natural logarithm of the spectral displacement corresponding to the damage state concerned. Φ refers to cumulative standard normal distribution function. Median spectral displacement values corresponding to each damage state, $S_{d,ds}$, are estimated in terms of story drift ratios specified for each building type.

On the other hand, the standard deviation β_{ds} is empirically estimated to cover the uncertainties associated with the definition of the damage level concerned, the building load capacity, and the earthquake ground motion specified. Once median story drift ratios are estimated for each building and for each damage state, the median spectral displacement value, $S_{d,ds}$, for the fundamental vibration mode is expressed as

$$S_{d,ds} = \alpha_2 D_{ds} H \quad (2)$$

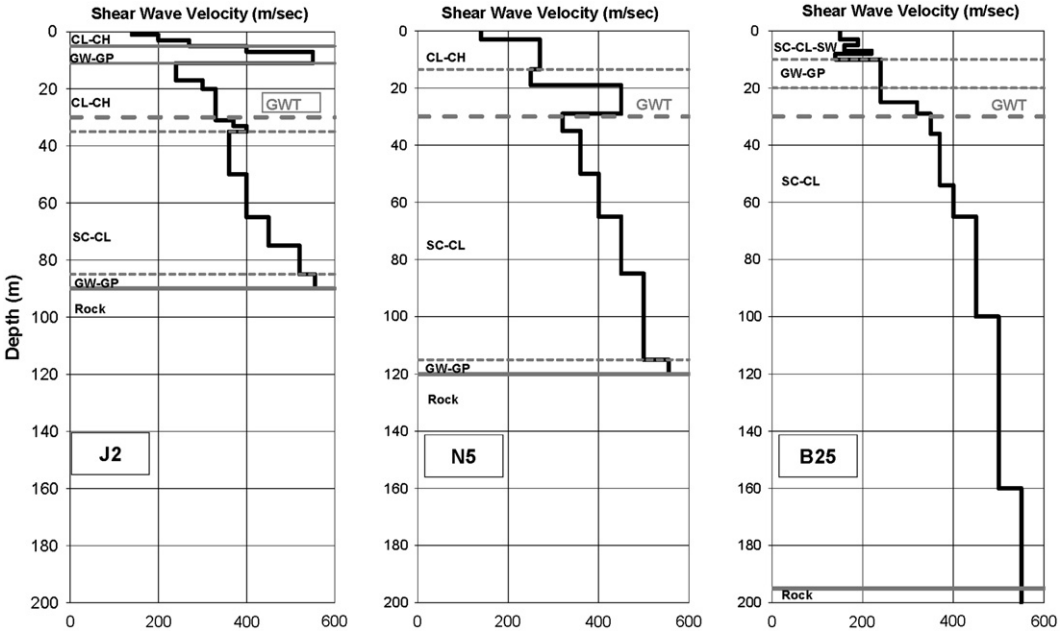

Fig. 2. Typical soil profiles and variation of shear wave velocity with depth in Zeytinburnu.

where D_{ds} refers to median storey drift ratio estimated for the damage state concerned, H represents the total building height, and α_2 is the modal parameter defined as

$$\alpha_2 = 1/(\Phi_{t,1}{}^{*}L_1) \quad (3)$$

where $\Phi_{t,1}$ represents the first mode shape amplitude at the building top and L_1 denotes the participation factor of the same mode. On the basis of selected classification system for a given building inventory, the values considered for H and α_2 as well as the median values of story drift ratios and spectral displacements defined in accordance with Eq. (2) are determined for each damage level specified, e.g., slight, moderate, extensive, and complete damage levels, respectively. Building damage is expressed in terms of number of buildings at each damage state for each building type at each cell in the grid system.

Vulnerability of pipeline inventory with respect to wave propagation is evaluated using site-specific PGV values as input parameters. Empirical correlations which relate damage rate to PGV are employed to predict damage in pipelines in terms of damage rate and number of pipe damages at each cell in the grid system. Results from vulnerability analyses are used to prepare damage distribution maps for the buildings and pipelines.

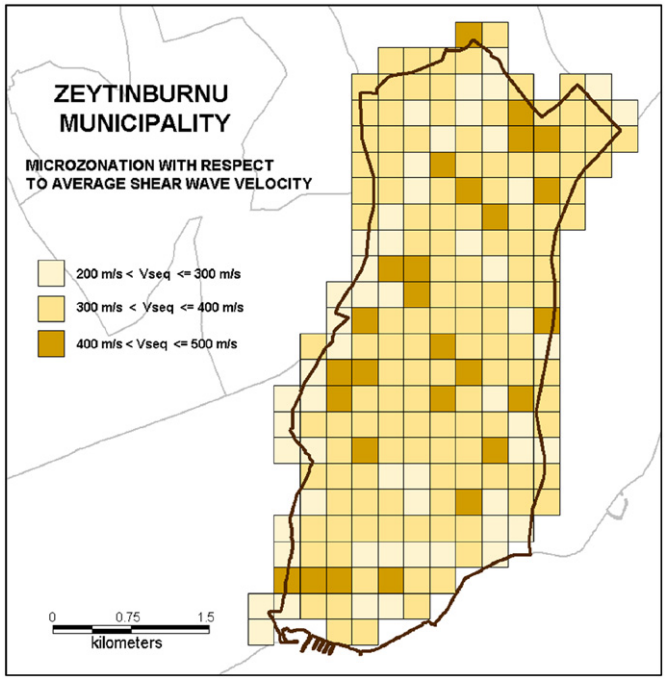

Fig. 3. Variation of average (equivalent) shear wave velocity for the top 30 m of soil profiles (V_{s30}).

Table 1
G/G_{max} and damping ratio–shear strain relationships used to define nonlinear soil properties.

Material type	Soil type	Reference
1	Fat clay (CH) PI=60%	Vucetic and Dobry [28]
2	Fat clay (CH) PI=45%	Vucetic and Dobry [28]
3	Lean clay (CL) PI=30%	Vucetic and Dobry [28]
4	Lean clay (CL) PI=15%	Vucetic and Dobry [28]
5	Silt (ML-MH) PI=10%	Darendeli [29]
6	Sand with fines (SM-SC)	Darendeli [29]
7	Clean sand (SW-SP)	Seed et al. [30]
8	Gravel (GM-GC)	Seed et al. [30]
9	Gravel (GW-GM)	Menq et al. [31]
10	Soft rock (0–6 m)	EPRI [32]
11	Soft rock (6–16 m)	EPRI [32]
12	Rock (16–37 m)	EPRI [32]
13	Rock (153–305 m)	EPRI [32]

3. Pilot study

The methodology is developed into a software package [21] to provide a practical tool for assessing the seismic vulnerability of an urban area. A pilot study is carried out using KoeriLossV2 to perform a damage scenario for Zeytinburnu district in Istanbul, Turkey, where building and gas pipeline inventories are available to some detail. The area of investigation is approximately 20 km^2 occupied mostly with low- to mid-rise residential buildings. The available inventory indicated that natural gas pipeline system in the district consists of steel pipes with diameters changing between 102 and 762 mm.

3.1. Seismic hazard and site response analyses

A grid system with cells of 250 m × 250 m is defined for the study area. Probabilistic seismic hazard analysis is carried out to

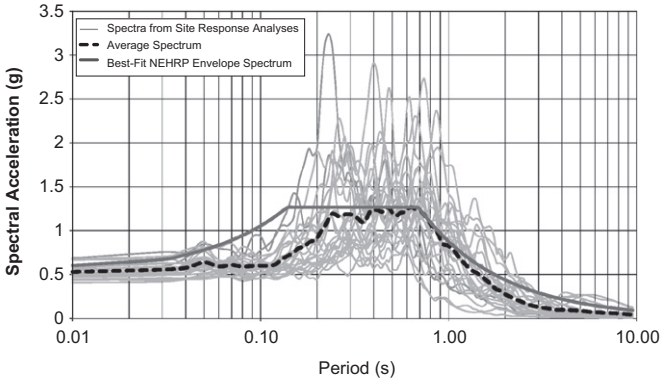

Fig. 4. Typical best-fit NEHRP envelope spectra fitted to average elastic acceleration response spectra, in comparison with the all acceleration response spectra calculated by site response analysis.

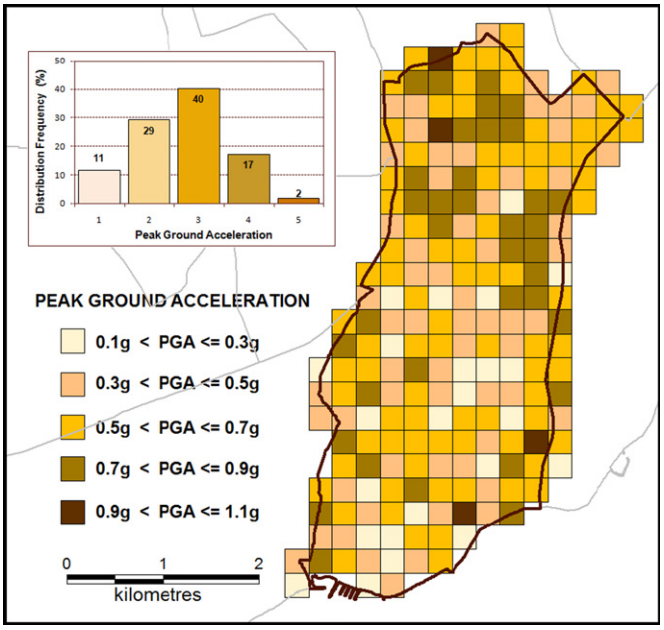

Fig. 5. Variation of peak ground acceleration (PGA) from site response analyses.

evaluate PGAs and spectral accelerations at $T=0.2$ and 1 s for each cell on the engineering bedrock outcrop [22]. A regional time dependent Poisson model for the return period of 475 years that corresponds approximately to 10% probability of exceedance in 50 years is considered in the analysis [23]. Twenty-four real acceleration time histories compatible with the earthquake hazard in terms of probable magnitude ($M=6.5$–7.5), epicenter distance ($R=20$–40 km), and fault mechanism (strike slip) recorded on stiff site conditions with average shear wave velocities (V_{s30}) larger than 420 m/s are selected as the probable input acceleration time histories from the PEER strong motion data bank [7]. Selected acceleration time histories are scaled with respect to PGAs estimated from the seismic hazard analysis for each cell before being used as outcrop motions in site response analyses. Scaled time histories for one cell are shown in Fig. 1.

The local site conditions are characterized based on an extensive site investigation study conducted in the area with at least one soil boring conducted at each cell location along with in-hole PS-Logging, surface seismic wave measurements and laboratory index tests [24]. All available information on geological and geotechnical conditions is evaluated to determine one representative soil profile with shear wave velocities extending down to engineering bedrock ($V_s \geq 750$ m/s) for each cell. Typical soil profiles obtained for Zeytinburnu are illustrated in Fig. 2. The variation V_{s30} in Zeytinburnu as determined from the detailed soil profiles is shown in Fig. 3. Empirical shear modulus and material damping ratio curves that were used to define dynamic properties of soil types are given in Table 1.

Site response analyses are performed for 24 acceleration time histories for the representative soil profiles in each cell using Shake91. The averages of 24 values of PGA, PGV, and acceleration response spectra from 24 Shake91 runs for each cell are

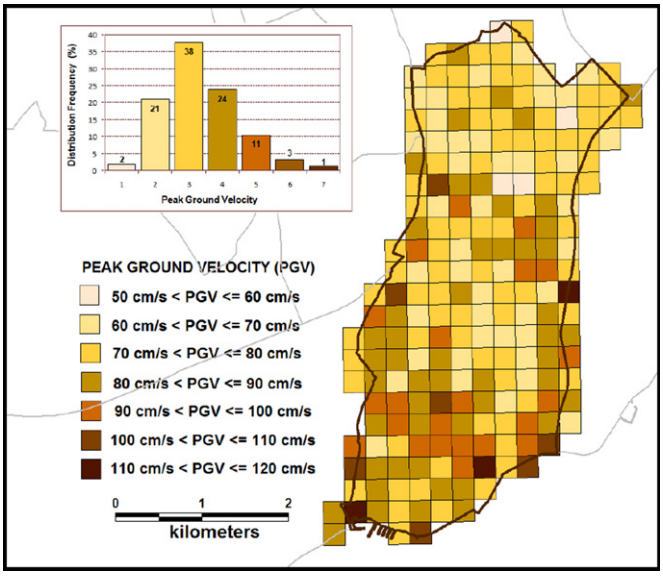

Fig. 6. Variation of peak ground velocity (PGV) from site response analyses.

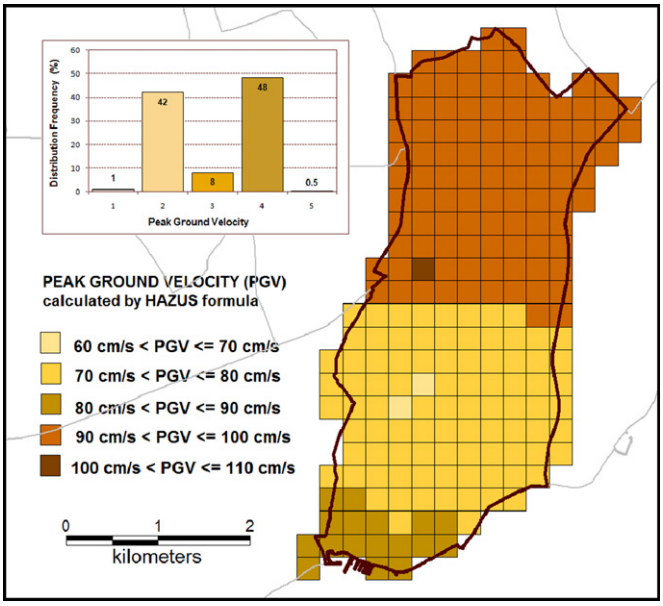

Fig. 8. Variation of peak ground velocity (PGV) by the Hazus formula using long period ($T=1$ s) spectral accelerations (S_1) estimated by NEHRP site amplification factors.

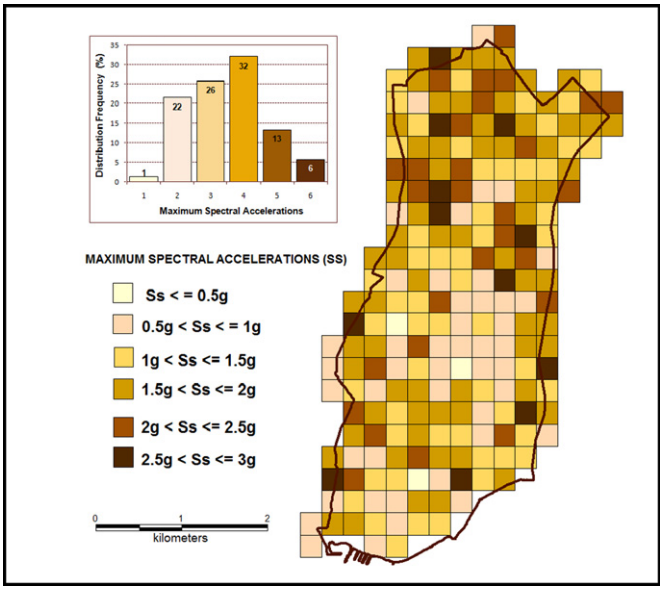

Fig. 7. Variation of short period ($T=0.2$ s) spectral accelerations (S_s) from site response analyses.

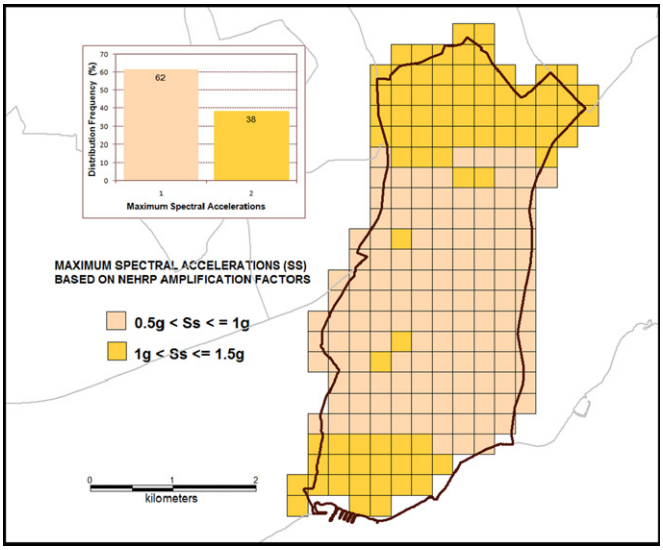

Fig. 9. Variation of short period ($T=0.2$ s) spectral accelerations (S_s) estimated by NEHRP site amplification factors.

determined to define the variation of ground shaking parameters due to the probabilistic seismic hazard scenario. The short and long period spectral accelerations (S_s and S_l) are obtained through optimization for the best-fit NEHRP envelope spectrum as shown in Fig. 4.

Resulting microzonation maps showing variations of site-specific PGA, PGV, and S_s values in Zeytinburnu are shown in Figs. 5–7, respectively, along with the distribution histograms. The variations of PGV and S_s can also be calculated empirically based on V_{s30}. S_s and S_l can be obtained by using the procedure proposed by Borcherdt [11] as suggested in NEHRP. PGV can be determined using Hazus formulation that relates S_l to PGV. Figs. 8 and 9 show variation of PGV, and S_s, respectively, as obtained through NEHRP based empirical procedures.

Comparisons of variations presented in Figs. 6 and 7 with those given in Figs. 8 and 9 show that the use of equivalent shear wave velocity to estimate the effects of site conditions may yield very different S_s and PGV amplitudes that may not always be on the

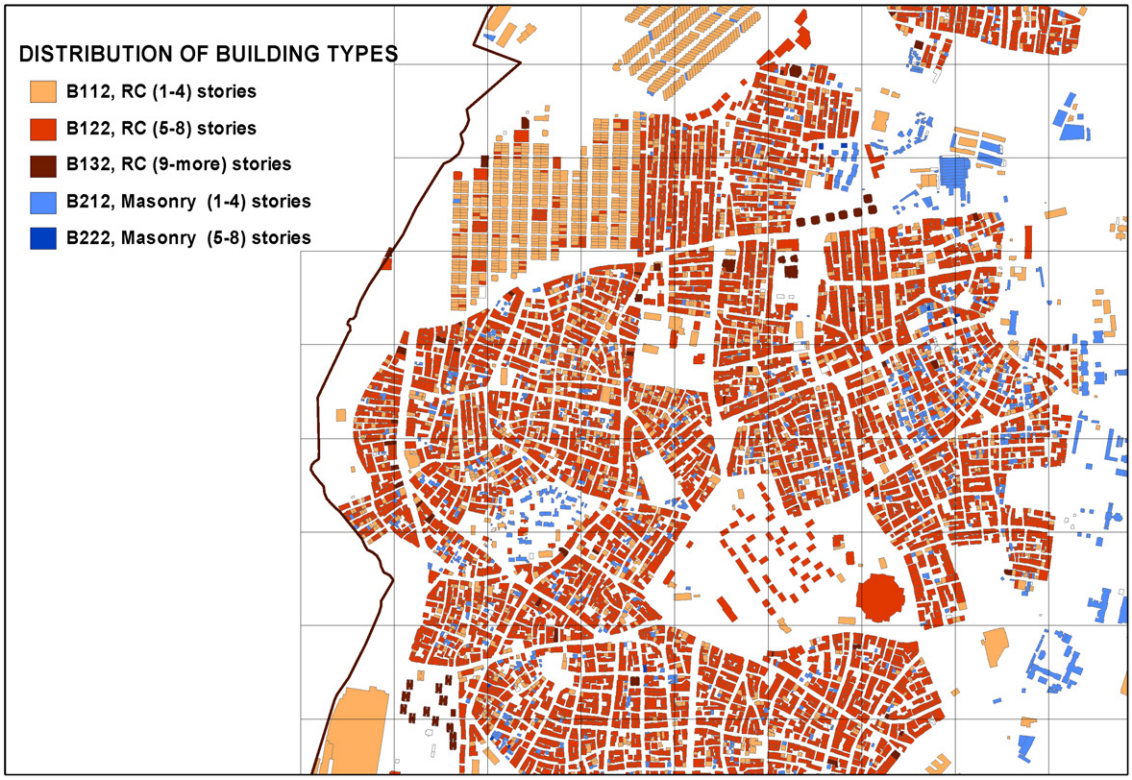

Fig. 10. Distribution of building types in Zeytinburnu.

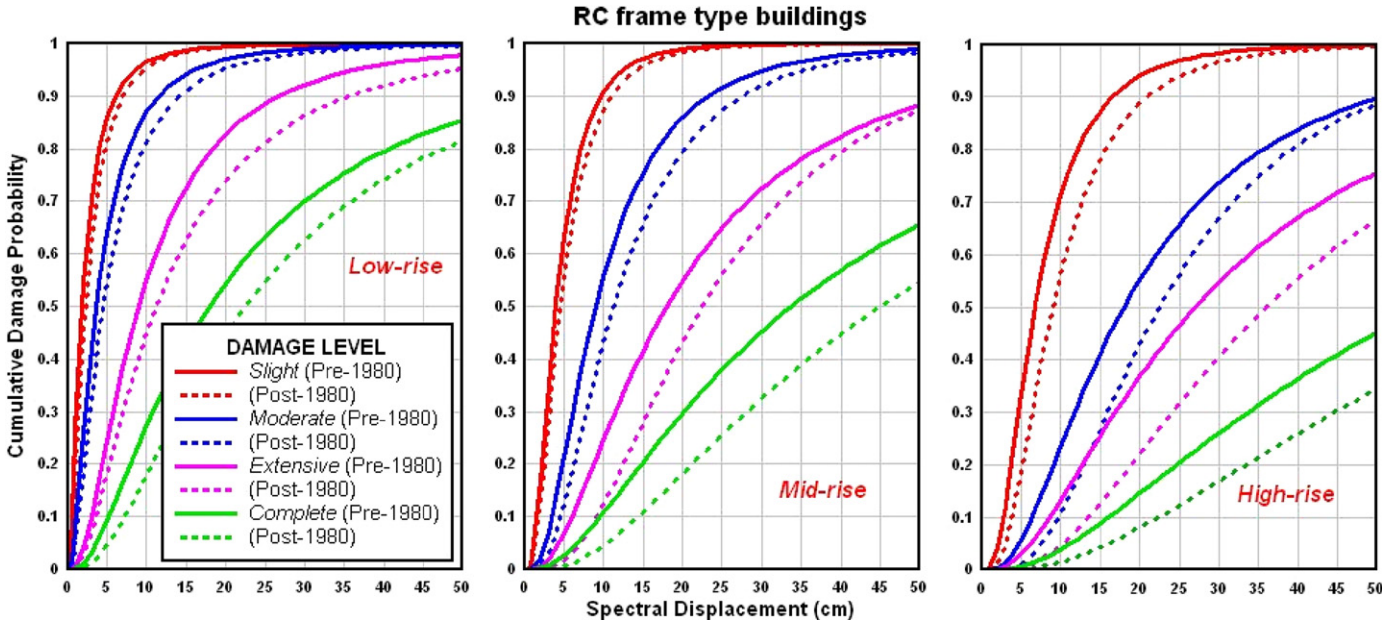

Fig. 11. Vulnerability relationships for reinforced concrete frame buildings.

Table 2
Damage distribution for different building types in Zeytinburnu.

Building type	Total number of buildings	Damage level (number of buildings)									
		None		Slight		Moderate		Extensive		Collapsed	
		SR	NH	SR	NH	SR	NH	SR	NH	SR	NH
RC low rise	3394	449	534	563	854	1054	1265	729	538	599	203
RC mid-rise	10,306	526	452	2236	3063	3707	3865	2384	1789	2083	1137
RC high rise (132)	144	4	7	31	49	34	37	39	31	35	21
Masonry low rise (212)	1821	238	262	359	476	444	514	357	334	423	235
Masonry mid-rise (222)	22	2	1	5	6	6	8	4	4	5	3
All	15,687	1219	1256	3194	4448	5245	5689	3513	2696	3145	1599

SR: using site response analysis; NH: using NEHRP amplification factors.

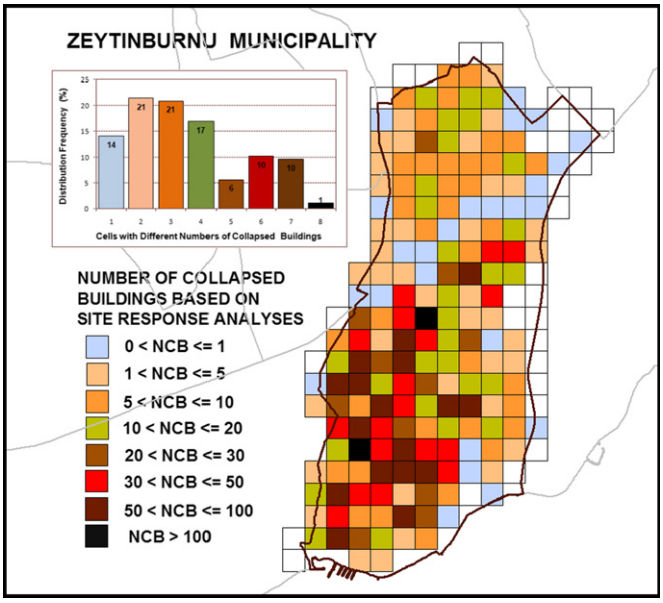

Fig. 12. Distribution of collapsed buildings in Zeytinburnu estimated using results of site response analyses.

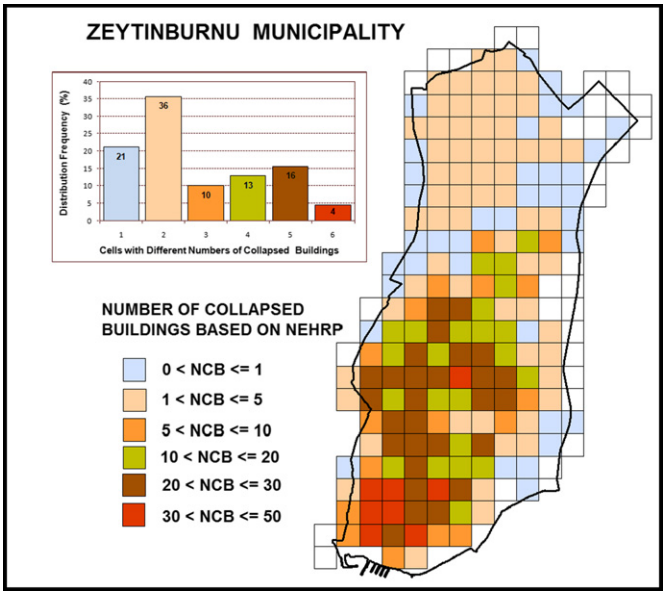

Fig. 13. Distribution of collapsed buildings in Zeytinburnu estimated using NEHRP factors.

safe side. The observed differences between Figs. 6 and 8 as well as between Figs. 7 and 9 indicate the importance of methodology employed in estimating the effects of site conditions.

3.2. *Vulnerability analyses for buildings and pipelines*

A detailed building inventory from street surveys for approximately 16,000 buildings is considered in the evaluation of seismic vulnerability of Zeytinburnu [25]. Building inventory is divided into groups based on the construction type, number of stories, and construction year of buildings [26,27]. All buildings are classified according to a 'Bijk' matrix where "i" shows the construction type as: (1) reinforced concrete frame building, (2) masonry building, (3) reinforced concrete shear wall buildings, and (4) precast building. The number of stories ("j" dimension of the matrix) is defined as: (1) low rise (1–4 stories, including basement), (2) mid-rise (5–8 stories, including basement), and (3) high-rise (8 or more stories, including basement). The construction date ("k" dimension of the matrix) is defined as: (1) construction year: pre-1980 and (2) construction year: post-1980. The building inventory classified according to 'Bijk' matrix in the town of Zeytinburnu is shown partly in Fig. 10. The available inventory in Zeytinburnu indicates that almost all of the buildings are mid-rise reinforced concrete frame buildings.

Region-specific vulnerability relationships [25] that relate spectral displacements to building damage for each building type are used to estimate damage in Zeytinburnu. Fig. 11 illustrates the displacement-based fragility curves for low-rise, mid-rise and high-rise reinforced concrete frame buildings constructed before and after 1980.

The distribution of number of buildings at each damage state for all building types in the area are computed and displayed in maps showing number of buildings at each cell for a given type of building and damage state. A summary of all results from damage evaluation is presented in Table 2. Numbers of buildings at each damage state estimated using NEHRP amplification factors are also given in Table 2 to provide direct comparisons.

Distribution of total number of collapsed buildings in Zeytinburnu obtained using site-specific ground shaking parameters is shown in Fig. 12. The variation of number of collapsed buildings estimated based on NEHRP amplification factors is given in Fig. 13.

A comparison of Figs. 12 and 13 clearly indicates that there are variations in the distribution of damage within the investigated region which cannot be detected when the site conditions and their effects are evaluated using NEHRP site classification and related amplification coefficients.

In order to demonstrate the extent of expected damage in Zeytinburnu, a representative damage ratio is calculated for each cell by

$$DR = \frac{(0^*N_{none} + 0.25^*N_{slight} + 0.50^*N_{moderate} + 0.75^*N_{extensive} + 1^*N_{collapse})}{(N_{none} + N_{slight} + N_{moderate} + N_{extensive} + N_{collapse})} \quad (4)$$

where N_{none}, N_{slight}, $N_{moderate}$, $N_{extensive}$ and $N_{collapse}$ are total number of buildings (includes all building types) at none, slight, moderate, extensive and collapsed damage states, respectively, within that particular cell. The variation of DR in Zeytinburnu is shown in Fig. 14.

The natural gas pipeline inventory of Zeytinburnu area is compiled based on information provided by Istanbul Gas Distribution Industry and Trade Co. Inc. (İGDAŞ). The inventory is consisted of length, diameter, and material properties of the main steel pipeline system. Empirical correlations listed in Table 3 that relates PGV to pipeline damage is used to estimate repair rate and number of repairs in the pipeline system due to wave propagation. Numbers of expected repairs at each cell are calculated as the product of repair rate and total pipeline length. Damage distribution maps showing the variation of repair rate is presented in Fig. 15.

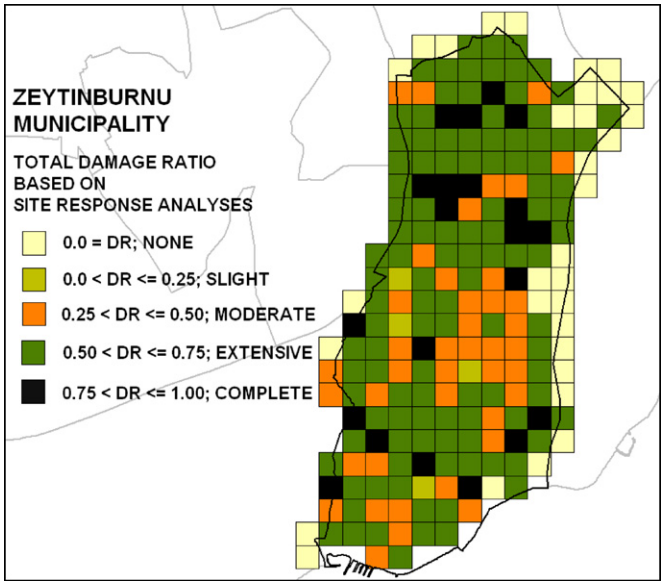

Fig. 14. Variation of total damage ratio representing the extent of damage for all building types in Zeytinburnu.

Table 3
Empirical pipeline vulnerability relations available in KoeriLossV2.

Empirical relation	Factors	Reference
RR (repair/km)=0.0001*K*PGV$^{2.25}$	PGV (cm/s), K: 1 if brittle material, K: 0.3 if ductile material	O'Rourke and Ayala [33]
RR(repair/1000 ft)=0.00032*K*PGV$^{1.93}$	PGV (in/s), K: coefficient depending on material type	Eidinger and Avila [34]
RR (repair/1000 ft)=0.00187*K*PGV	PGV (in/s), K: coefficient depending on material type	ALA [35]
RR(repair/km) =K*513*PGS$^{0.89}$	PGV (cm/s), PGS=ground strain, K: 1 if brittle material, K: 0.3 if ductile material	O'Rourke and Deyoe [36]

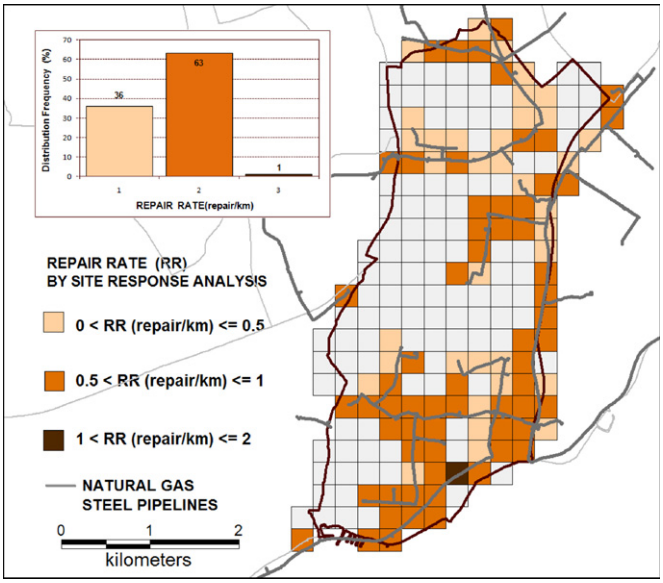

Fig. 15. Distribution of predicted repair rate in natural gas pipeline system in Zeytinburnu.

4. Simplified versus site response analysis

The comparison between the spectral accelerations calculated from site response analyses using the best envelope fitting procedure with those values calculated by the NEHRP formulation indicates that the values obtained by site response analyses have much larger scatter as shown in Fig. 16. The difference in the data range is much more significant for short period spectral acceleration values.

Larger scatter observed in the results obtained from site response analyses may be the indication of more accurate determination of site effects. NEHRP site classification based on equivalent shear wave velocity yields only two site classes in the case of Zeytinburnu. This is partly due to the fact that shear wave velocity ranges used in the NEHRP site classes are defined within relatively large ranges.

The variability of the calculated parameters to be used for the vulnerability assessment of the building stock is an important factor. Considering the variability taken into account by assigning different earthquake characteristics for each cell and the differences in the soil profiles, it appears logical to use the spectral acceleration values obtained from site response analysis for the vulnerability assessment. However, it is also possible to argue that the sophistication introduced during this process may not always give more correct or accurate results. In addition, the decision of using one of the spectral accelerations determined by best envelope approach would play a very important role on the amplitude of the estimated vulnerability of the building stock.

A similar comparison can also be made with respect to PGV values that could be an important parameter in estimating damage distribution in pipeline systems. As can be seen in Fig. 17, the difference is significant with PGV values calculated by the Hazus formula being almost always lower than those calculated from site response analysis.

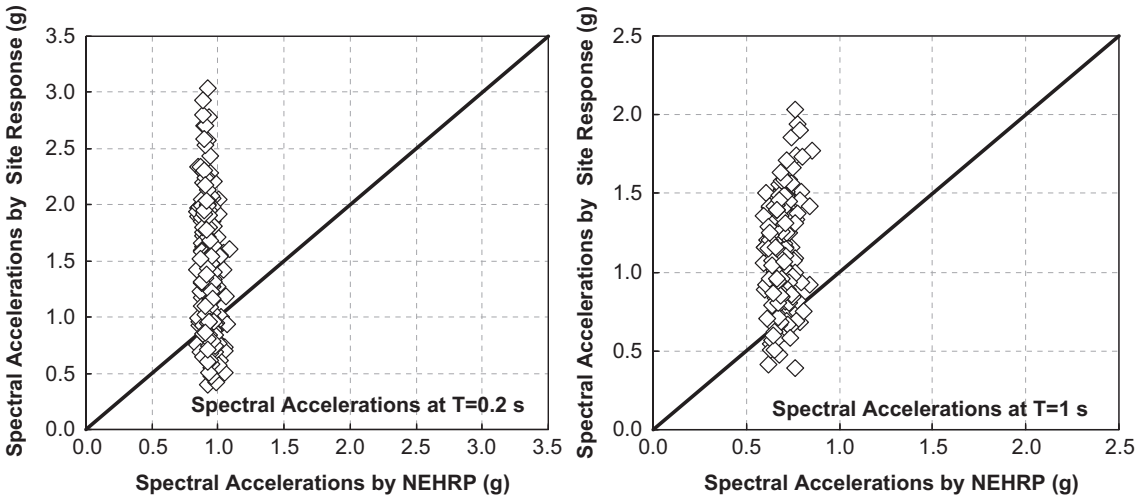

Fig. 16. Correlation between short and long period spectral accelerations (S_s and S_1) calculated by site response analyses and by using the empirical approach of NEHRP.

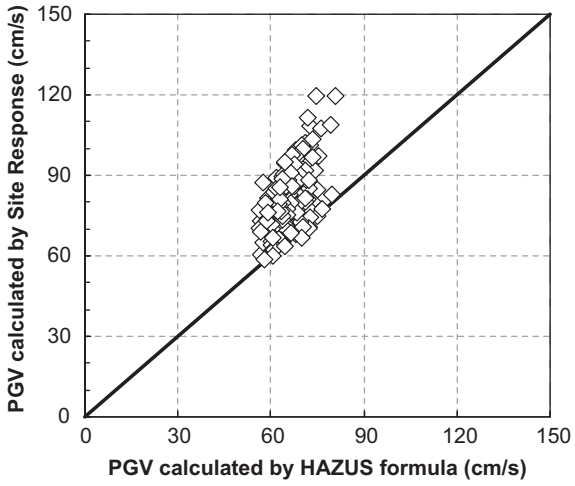

Fig. 17. Correlation between peak ground velocities (PGV) calculated by site response analyses and by using the empirical formulation of Hazus.

5. Conclusions

A methodology for performing urban damage scenarios for buildings and pipeline networks where local site conditions are taken into account by performing large number of 1D site-specific ground response analyses is presented. The methodology is developed into a software tool and application to a district in Istanbul, Turkey demonstrated that there are significant variations in the ground motion parameters within the investigated region which cannot be detected when the site conditions and their effects are evaluated using NEHRP site classification and related amplification coefficients. Therefore, it appears essential to perform site response analyses to have more accurate information on ground shaking characteristics for microzonation and for the estimation of seismic damage in buildings and lifeline systems.

Acknowledgements

The authors would like to acknowledge the support and contributions of all their colleagues in the Earthquake Engineering Department of Kandilli Observatory and Earthquake Research Institute, specifically of, Prof. M. Erdik, Prof. N. Aydınoğlu, Prof. E. Durukal, M. Demircioğlu, Dr. K. Şeşetyan, and U. Hancılar.

References

[1] Hazus. Earthquake loss estimation methodology. Technical manual. Washington, DC, USA: Federal Emergency Management Agency and National Institute of Buildings Sciences; 2003.
[2] Zonno G, Garcia-Fernandez M, Jimenez MJ, Menoni S, Meroni1 F, Petrini V. The SERGISAI procedure for seismic risk assessment. Journal of Seismology 2003;**7**:259–77.
[3] RISK-UE. An advanced approach to earthquake risk scenarios with applications to different European towns: synthesis of the application to Thessaloniki city, Pitilakis K, A., RISK-UE report, 2004.
[4] Sousa ML, Campos Costa A, Carvalho A, Coelho E. An automatic seismic scenario loss methodology integrated on a geographic information system. In: 13th world conference on earthquake engineering, Vancouver, BC, Canada, August 1–6, Paper no. 2526, 2004.
[5] Molina-Palacios S, Lindholm CD. SELENA V1.0 user and technical manual. Norway: NORSAR; 2006. 〈http://www.norsar.no/seismology/selena.html〉.
[6] Idriss IM, Sun JI. Shake91, a computer program for conducting equivalent linear seismic response analysis of horizontally layered soil deposits modified based on the original SHAKE program published in December 1972 by Schnabel, Lysmer and Seed, 1992.
[7] Ansal A, Tönük G. Source and site effects for microzonation. In: Pitilakis K, editor. Theme lecture, 4th International Conference on Earthquake Geotechnical Engineering, Earthquake Geotechnical Engineering, Springer; 2007. p. 73–92 [Chapter 4].
[8] Ansal A, Akinci G, Cultrera M, Erdik V, Pessina G, Tonuk G, et al. Loss estimation in Istanbul based on deterministic earthquake scenarios of the Marmara Sea Region (Turkey). Soil Dynamics and Earthquake Engineering 2009;29(4):699–709.
[9] Ansal A, Durukal E, Tönük G. Selection and scaling of real acceleration time histories for site response analyses. In: Proceedings of the ISSMGE ETC12 Athens Workshop, Athens, Greece, 2006.
[10] Durukal E, Ansal A, Tönük G. Effect of ground motion scaling and uncertainties in site characterisation on site response analyses. In: Proceedings of the 100th Anniversary Earthquake Conference Commemorating the 1906 San Francisco Earthquake, San Francisco, USA, 2006.
[11] Borcherdt RD. Estimates of site dependent response spectra for design (methodology and justification). Earthquake Spectra 1994;10(4):617–654.
[12] Ansal A, Laue J, Buchheister J, Erdik M, Springman SM, Studer J, et al. Site characterization and site amplification for a seismic microzonation study in Turkey. In: Proceedings of the 11th International Conference on Soil Dynamics and Earthquake Engineering and 3rd Earthquake Geotechnical Engineering, San Francisco, USA, 2004.
[13] NEHRP. Recommended provisions for new buildings and other structures, FEMA-450, prepared by the Building Seismic Safety Council for the Federal Emergency Management Agency, Washington, DC, 2003.
[14] Ansal A, Tönük G, Demircioglu M, Bayraklı Y, Sesetyan K, Erdik M. Ground motion parameters for vulnerability assessment. In: Proceedings of the First European Conference on Earthquake Engineering and Seismology, Geneva, Switzerland, Paper number: 1790, 2006.
[15] Erdik M, Fahjan Y. System analysis and risk. In: Oliveira CS, Roca A, Goula X, editors. Assessing and managing earthquake risk geo-scientific and engineering knowledge for earthquake risk mitigation: developments, tools,

techniques, Part 3, Book series: Geotechnical, Geological, and earthquake engineering, vol. 2, 2005.
[16] Ansal A, Erdik M, Studer J, Springman S, Laue J, Buchheister J, et al.. Seismic microzonation for earthquake risk mitigation in Turkey. In: Proceedings of the 13th World Conference of Earthquake Engineering, Vancouver, CD paper no. 1428, 2004.
[17] ATC & SSC. ATC-40 seismic evaluation and retrofit of concrete buildings. Report SSC 96-01, California, EUA, 1996.
[18] FEMA273. NEHRP commentary on the guidelines for the seismic rehabilitation of buildings. SW Washington, DC, USA: Federal Emergency Management Agency; 1997.
[19] FEMA 356. Prestandard and commentary for the seismic rehabilitation of buildings. Washington, DC, USA: Federal Emergency Management Agency; 2000.
[20] Kircher CA, Nassar AA, Kustu O, Holmes WT. Development of building damage functions for earthquake loss estimation. Earthquake Spectra 1997;13(4):663–82.
[21] KoeriLossV2. Earthquake disaster scenario prediction and loss modelling for urban areas. In: Spence R, editor. EU FP6 project on risk mitigation for earthquakes and landslides report, 2007.
[22] Erdik M, Demircioglu M, Sesetyan K, Durukal E. Assessment of earthquake hazard for Bakırköy, Gemlik, Bandırma, Tekirdağ and Körfez, WB MEER project -A3 component, microzonation and hazard vulnerability studies for disaster mitigation in pilot municipalities, Bogazici University, Kandilli Observatory and Earthquake Engineering Research Institute, 2005.
[23] Erdik M, Demircioglu M, Sesetyan K, Durukal E, Siyahi B. Earthquake hazard in Marmara region. Soil Dynamics and Earthquake Engineering 2004;24:605–31.
[24] OYO Inc., Japan. Production of microzonation report and maps on European side (south). Final report to Istanbul Metropolitan Municipality, 2007.
[25] Aydınoglu N, Polat Z. First level evaluation and assessment of building earthquake performance. Report for the Istanbul Master Plan Zeytinburnu Pilot Project, Metropolitan Municipality of Istanbul, Planning and Construction Directorate, 2004 [in Turkish].
[26] Erdik M, Aydınoglu N, Barka A, Yüzügüllü Ö, Siyahi B, Durukal E, et al. BU-ARC, earthquake risk assessment for Istanbul metropolitan area, project report. Bogazici University Publication; 2002.
[27] Erdik M, Aydinoglu N, Fahjan Y, Sesetyan K, Demircioglu M, Siyahi B, et al. Earthquake risk assessment for Istanbul metropolitan area. Earthquake Engineering & Engineering Vibration 2003;2(1):1–25.
[28] Vucetic M, Dobry R. Effect of soil plasticity on cyclic response. Journal of Geotechnical Engineering, ASCE 1991;117(1):89–107.
[29] Darendeli MB. A new family of normalized modulus reduction and material damping curves. PhD thesis, Civil Engineering Department, University of Texas at Austin, 2001.
[30] Seed HB, Wong RT, Idriss IM, Tokimatsu K. Moduli and damping factors for dynamic analysis of cohesionless soils. Journal of Geotechnical Engineering 1986;112(11):1016–32.
[31] Menq FY, Stokoe KH, Kavazanjian E. Linear dynamic properties of sandy and gravelly soils from largescale resonant tests. In: International symposium IS Lyon 03, deformation characteristics of geomaterials, Lyon, France, 22–24 September 2003.
[32] EPRI. Guidelines for determining design basis ground motions, vol. 1, Palo Alto, CA, Electric Power Research Institute, EPRI TR-102293, 1993.
[33] O'Rourke M, Ayala G. Pipeline damage due to wave propagation. Journal of Geotechnical Engineering 1993;119(9):1490–8.
[34] Eidinger J, Avila E. Guidelines for the seismic upgrade of water transmission facilities. Monograph no. 15, TCLEE/ASCE, 1999.
[35] ALA (American Lifelines Alliance). Seismic fragility formulations for water systems, part 1—guideline, 2001. 〈http://www.americanlifelinesalliance.org〉.
[36] O'Rourke M, Deyoe E. Seismic damage to segmented buried pipe. Earthquake Spectra 2004;20:1167–83.